J|A|C|S
ARTICLES
Published on Web 02/25/2005

Magnetic Field Effects on Bioelectrocatalytic Reactions of Surface-Confined Enzyme Systems: Enhanced Performance of Biofuel Cells

Eugenii Katz, Oleg Lioubashevski, and Itamar Willner*

Contribution from the Institute of Chemistry, The Hebrew University of Jerusalem, Jerusalem 91904, Israel

Received September 26, 2004; E-mail: willnea@vms.huji.ac.il

Abstract: The effect of a constant magnetic field on bioelectrocatalytic transformations of three different enzyme assemblies linked to electrodes is examined and correlated with a theoretical magnetohydrodynamic model. The systems consist of surface-reconstituted glucose oxidase (GOx), an integrated lactate dehydrogenase/nicotinamide/pyrroloquinoline quinone assembly (LDH/NAD^+-PQQ), and a cytochrome *c*/cytochrome oxidase system (Cyt *c*/COx) linked to the electrodes. Pronounced effects of a constant magnetic field applied parallel to the electrode surface are observed for the bioelectrocatalyzed oxidation of glucose and lactate by the GOx-electrode and LDH/NAD^+-PQQ-electrode, respectively. The enhancement of the bioelectrocatalytic processes correlates nicely with the magnetohydrodynamic model, and the limiting current densities (i_L) relate to $B^{1/3}$ (B = magnetic flux density) and to $C^{*4/3}$ (C^* = bulk concentration of the substrate). A small magnetic field effect is observed for the Cyt *c*/COx-electrode, and its origin is still questionable. The effect of the constant magnetic field on the performance of biofuel cells with different configurations is examined. For the biofuel cell consisting of LDH/NAD^+-PQQ anode and Cyt *c*/COx cathode, a 3-fold increase in the power output was observed at an applied magnetic field of $B = 0.92$ T and external load of 1.2 kΩ.

Introduction

Electrical contacting of redox enzymes with electrode supports attracts substantial research efforts directed to the development of biosensors,[1,2] bioelectrocatalyzed chemical transformations,[3] and the development of biofuel cell elements.[4,5] Tethering of electroactive relays to redox proteins[6] or the immobilization of redox proteins in electroactive polymers associated with electrodes[7] are common practices to electrically contact and activate the redox enzymes. Recently, we reported on the effective electrical wiring of redox enzymes with electrodes by their structural alignment on conductive supports through the surface reconstitution of apo-flavoenzymes or apo-pyrroloquinoline quinone (PQQ)-dependent enzymes on a relay-FAD monolayer assembly[8] or a redox polymer-PQQ thin film[9] linked to electrodes, respectively. This concept was further generalized by tailoring integrated, electrically contacted, cofactor-dependent enzyme electrodes by the cross-linking of affinity complexes between NAD^+-dependent enzymes and an electrocatalyst-NAD^+ monolayer[10] or thin film[11] associated with electrodes.

(1) (a) Willner, I.; Katz, E. *Angew. Chem., Int. Ed.* **2000**, *39*, 1180−1218. (b) Willner, I.; Katz, E.; Willner, B. In *Biosensors and Their Applications*; Yang, V. C., Ngo, T. T., Eds.; Kluwer Academic Publishers: New York, 2000; Chapter 4, pp 47−98. (c) Katz, E.; Shipway, A. N.; Willner, I. In *Bioelectrochemistry;* Wilson, G. S., Bard, A. J., Stratmann, M., Eds.; Encyclopedia of Electrochemistry, Vol. 9; Wiley-VCH: Weinheim, Germany, 2002; Chapter 17, pp 559−626. (d) Katz, E.; Shipway, A. N.; Willner, I. In *Electron Transfer in Chemistry*; Balzani, V., Ed.; Vol. 4; Wiley-VCH: Weinheim, Germany, 2001; pp 127−201.

(2) (a) Bartlett, P. N.; Tebbutt, P.; Whitaker, R. C. *Prog. React. Kinet.* **1991**, *16*, 55−155. (b) Heller, A. *Acc. Chem. Res.* **1990**, *23*, 128−134. (c) Armstrong, F. A.; Wilson, G. S. *Electrochem. Acta* **2000**, *45*, 2623−2645. (d) Habermuller, L.; Mosbach, M.; Schuhmann, W. *Fresenius J. Anal. Chem.* **2000**, *366*, 560−568. (e) Armstrong, F. A.; Heering, H. A.; Hirst, J. *Chem. Soc. Rev.* **1997**, *26*, 169−179.

(3) Laane, C.; Pronk, W.; Fraseen, M.; Veeger, C. *Enzyme Microb. Technol.* **1984**, *6*, 165−168.

(4) (a) Katz, E.; Willner, I.; Kotlyar, A. B. *J. Electroanal. Chem.* **1999**, *479*, 64−68. (b) Willner, I.; Arad, G.; Katz, E. *Bioelectrochem. Bioenerg.* **1998**, *44*, 209−214. (c) Willner, I.; Katz, E.; Patolsky, F.; Bückmann, A. F. *J. Chem. Soc., Perkin Trans. 2* **1998**, 1817−1822. (d) Katz, E.; Filanovsky, B.; Willner, I. *New J. Chem.* **1999**, *23*, 481−487. (e) Katz, E.; Shipway, A. N.; Willner, I. In *Handbook of Fuel Cell Technology*; Vielstich, W., Gasteiger, H., Eds.; Willey, Chichester, 2002; Vol. 1, Part 4, Chapter 21, pp 355−381. (f) Katz, E. In *2004 Yearbook of Science and Technology*; Blumel, D., Ed.; McGraw-Hill Professional: New York, 2004; pp 33−37.

(5) (a) Palmore, G. T. R.; Bertschy, H.; Bergens, S. H.; Whitesides, G. M. *J. Electroanal. Chem.* **1998**, *443*, 155−161. (b) Tsujimura, S.; Tatsumi, H.; Ogawa, J.; Shimizu, S.; Kano, K.; Ikeda, T. *J. Electroanal. Chem.* **2001**, *496*, 69−75. (c) Tsujimura, S.; Fujita, M.; Tatsumi, H.; Kano, K.; Ikeda, T. *Phys. Chem. Chem. Phys.* **2001**, *3*, 1331−1335. (d) Chen, T.; Barton, S. C.; Binyamin, G.; Gao, Z. Q.; Zhang, Y. C.; Kim, H. H.; Heller, A. *J. Am. Chem. Soc.* **2001**, *123*, 8630−8631. (e) Mano, N.; Mao, F.; Heller, A. *J. Am. Chem. Soc.* **2002**, *124*, 12962−12963. (f) Heller, A. *Phys. Chem. Chem. Phys.* **2004**, *6*, 209−216.

(6) (a) Schuhmann, W.; Ohara, T. J.; Schmidt, H.-L.; Heller, A. *J. Am. Chem. Soc.* **1991**, *113*, 1394−1397. (b) Willner, I.; Riklin, A.; Shoham, B.; Rivenzon, D.; Katz, E. *Adv. Mater.* **1993**, *5*, 912−915.

(7) (a) Heller, A. *J. Phys. Chem.* **1992**, *96*, 3579−3587. (b) Willner, I.; Willner, B. *React. Polym.* **1994**, *22*, 267−279.

(8) (a) Willner, I.; Heleg-Shabtai, V.; Blonder, R.; Katz, E.; Tao, G.; Bückmann, A. F.; Heller, A. *J. Am. Chem. Soc.* **1996**, *118*, 10321−10322. (b) Katz, E.; Riklin, A.; Heleg-Shabtai, V.; Willner, I.; Bückmann, A. F. *Anal. Chim. Acta* **1999**, *385*, 45−58. (c) Zayats, M.; Katz, E.; Willner, I. *J. Am. Chem. Soc.* **2002**, *124*, 2120−2121.

(9) Raitman, O. A.; Patolsky, F.; Katz, E.; Willner, I. *Chem. Commun.* **2002**, 1936−1937.

(10) (a) Bardea, A.; Katz, E.; Bückmann, A. F.; Willner, I. *J. Am. Chem. Soc.* **1997**, *119*, 9114−9119. (b) Katz, E.; Heleg-Shabtai, V.; Bardea, A.; Willner, I.; Rau, H. K.; Haehnel, W. *Biosens. Bioelectron.* **1998**, *13*, 741−756.

(11) Raitman, O. A.; Katz, E.; Bückmann, A. F.; Willner, I. *J. Am. Chem. Soc.* **2002**, *124*, 6487−6496.

Recently, metal nanoparticles[12] or carbon nanotubes[13] were employed as efficient electrical contacting elements of glucose oxidase by the reconstitution of the apo-enzyme on the FAD cofactor-functionalized Au nanoparticles or carbon nanotubes, respectively. In these systems, the direct electron transfer from the enzyme cofactor to the conductive support proceeds through the conductive nano-objects. Also, the reconstitution of apo-glucose oxidase on FAD-modified polyaniline wires wrapped around a DNA template associated with an electrode led to an electrically contacted enzyme electrode.[14]

Efficient electron transfer between redox enzymes and conductive electrode supports as a result of structural alignment and optimal positioning of the electron mediators allowed development of noncompartmentalized biofuel cells.[15] Cross-reactions of the anolyte fuel and catholyte oxidizer with the opposite electrodes were prevented because of the high specificity of the bioelectrocatalytic reactions at the electrodes, and thus the use of a membrane separating the catholyte and anolyte solutions could be eliminated. These biofuel cells were suggested as future implantable batteries that use glucose in blood as the fuel source[4a,5f,15] and as self-powered biosensors for glucose or lactate, since the output voltage and current signals are dependent on the substrate concentration.[16]

Magnetic field could affect the rate of electrochemical reactions through the magnetohydrodynamic effect. This effect was well documented for simple one-step electrochemical reactions involving inorganic (e.g., ferrocyanide) or organic (e.g., acetophenone) compounds.[17] Recently, we developed the theoretical approach to account the magnetohydrodynamic effect on electrochemical processes.[18] The effect of a constant magnetic field on bioelectrochemical systems was also demonstrated by us for the first time, using cyctochrome *c*-based electrochemical systems as examples.[19] We have studied the magnetic field effect on cytochrome *c*-mediated biocatalytic processes, and the enhanced bioelectrocatalytic processes correlated nicely with the magnetohydrodynamic model that was developed. In these systems, all components participating in the bioelectrocatalytic processes, including cytochrome *c*, operating as a redox mediator, and the enzymes (cytochrome oxidase or lactic dehydrogenase), communicating with cytochrome *c*, were solubilized in the electrolyte solution as diffusional components. In the present paper, we report new results on the enhancement of bioelectrocatalytic processes of the surface-integrated biocatalytic systems by the magnetohydrodynamic effect. Specifically, we examine the effect of a constant magnetic field on the performance of biofuel cells and demonstrate the enhancement of the electrical output of the biofuel cells as a result of the magnetohydrodynamic effect.

Experimental Section

Chemicals. Glucose oxidase (GOx, EC 1.1.3.4 from *Aspergillus niger*) and L-lactic dehydrogenase (LDH, EC 1.1.1.27 from rabbit muscle, type II) were purchased from Sigma and used without further purification. Apo-glucose oxidase (apo-GOx) was prepared by a modification[8b] of the reported method.[20] Cytochrome oxidase (COx) was isolated from a Keilin−Hartree heart muscle and purified according to a published technique.[21] Yeast iso-2-cytochrome *c* (Cyt *c*) from *Saccharomyces cerevisiae* (Sigma) was purified by ion-exchange chromatography. N^6-(2-Aminoethyl)-flavin adenine dinucleotide (N^6-(2-aminoethyl)-FAD, **2**)[22] and N^6-(2-aminoethyl)-β-nicotinamide adenine dinucleotide (N^6-(2-aminoethyl)-NAD^+, **3**)[23] were synthesized and purified as described before. All other chemicals, including pyrroloquinoline quinone (PQQ, **1**), *N*-succinimidyl-3-maleimidopropionate (**4**), 4-(2-hydroxyethyl)piperazine-1 ethanesulfonic acid sodium salt (HEPES), tris(hydroxymethyl)aminomethane hydrochloride (TRIS), 1-ethyl-3-(3-dimethylaminopropyl)carbodiimide (EDC), glutaric dialdehyde, β-D-(+)-glucose, and sodium L-lactate were purchased from Sigma and Aldrich and used as supplied. Ultrapure water from Barnstead NANOpure Diamond system was used in all experiments.

Modification of Electrodes and Design of the Electrochemical Cells. Glass supports (10 × 10 mm) coated with a chromium sublayer (~5 nm) and a gold layer (~50 nm) supplied by Analytical-μSystem (Germany) were used as working electrodes. The Au electrodes were cleaned in boiling ethanol for 2 min, and then they were thoroughly rinsed with water. Cystamine was self-assembled on the electrodes to yield the amino-functionalized surface as described before.[24] The resulting amino-functionalized Au electrodes were reacted with PQQ (**1**) as described before to generate the PQQ-monolayer-functionalized electrodes.[24b,c] The covalent coupling of the N^6-(2-aminoethyl)-FAD (**2**) to the PQQ-modified electrode was performed by soaking the electrode in the 0.1 M HEPES-buffer solution (pH = 7.2) containing 5×10^{-4} M (**2**) and 5×10^{-3} M EDC for 2 h at room temperature. The PQQ-FAD-functionalized electrode was reacted with 1 mg·mL^{-1} apo-GOx in 0.1 M phosphate buffer, pH = 7.0, for 5 h at room temperature. The modified electrode was washed with water to yield the GOx-reconstituted electrodes for biocatalytic oxidation of glucose.[8] The covalent coupling of the N^6-(2-aminoethyl)-NAD^+ (**3**) to the PQQ-modified electrode was performed by soaking the electrode in the 0.1 M HEPES-buffer solution (pH = 7.2) containing 5×10^{-4} M (**3**) and 5×10^{-3} M EDC for 2 h at room temperature. The PQQ-NAD^+-functionalized electrode was reacted with 1 mg·mL^{-1} LDH in 0.1 M phosphate buffer, pH = 7.0, for 5 h at room temperature, briefly washed with the phosphate buffer, and reacted with an aqueous glutaric dialdehyde solution, 10% (v/v), for 30 min at room temperature. The resulting electrode was rinsed with water to yield the LDH/NAD^+-PQQ-integrated electrode for biocatalytic oxidation of lactate.[10a] The iso-2-cytochrome *c* (Cyt *c*) was covalently linked in a monolayer configuration to the Au electrode. The amino-functionalized Au surface was reacted with *N*-succinimidyl-3-maleimidopropionate (**4**) in 0.1 M HEPES-buffer, pH = 7.2, for 2 h, followed by rinsing with water. The maleimide-functionalized electrode was treated with Cyt *c* solution,

(12) Xiao, Y.; Patolsky, F.; Katz, E.; Hainfeld, J. F.; Willner, I. *Science* **2003**, *299*, 1877−1881.
(13) Patolsky, F.; Weizmann, Y.; Willner, I. *Angew. Chem., Int. Ed.* **2004**, *43*, 2113-2117.
(14) Shi, L.; Xiao, Y.; Willner, I. *Electrochem. Commun.* **2004**, *6*, 1057−1060.
(15) Katz, E.; Willner, I. *J. Am. Chem. Soc.* **2003**, *125*, 6803−6813.
(16) Katz, E.; Bückmann, A. F. Willner, I. *J. Am. Chem. Soc.* **2001**, *123*, 10752−10753.
(17) (a) Fahidy, T. Z. *Electrochim. Acta* **1973**, *18*, 607−614. (b) Aogaki, R.; Fueki, K.; Mukaibo, T. *Denki Kagaku* **1976**, *44*, 89−94. (c) Aogaki, R., Fueki, K.; Mukaibo, T. *Denki Kagaku* **1975**, *43*, 504−508. (d) Ragsdale, S. R.; Lee, J.; Gao, X. P.; White, H. S. *J. Phys. Chem.* **1996**, *100*, 5913−5922. (e) Ragsdale, S. R.; Lee, J. H.; White, H. S. *Anal. Chem.* **1997**, *69*, 2070−2076. (f) Leventis, N.; Chen, M. G.; Gao, X. R.; Canalas, M.; Zhang, P. *J. Phys. Chem. B* **1998**, *102*, 3512−3522.
(18) Lioubashevski, O.; Katz, E.; Willner, I. *J. Phys. Chem. B* **2004**, *108*, 5778−5784.
(19) Katz, E.; Lioubashevski, O.; Willner, I. *J. Am. Chem. Soc.* **2004**, *126*, 11088−11092.
(20) Morris, D. L.; Buckler, R. T. In *Methods in Enzymology*; Langone, J. J., Van Vunakis, H., Eds.; Academic Press: Orlando, FL, 1983; Vol. 92, Part E, pp 413−417.
(21) Yonetani, T. *J. Biol. Chem.* **1961**, *236*, 1680−1688.
(22) Bückmann, A. F.; Wray, V.; Stocker, A. In *Methods in Enzyhmology: Vitamins and Coenzymes*; McCormick, D. B., Ed.; Academic Press: Orlando, Fl, 1997; Vol. 280, Part 1, p 360.
(23) Bückmann, A. F.; Wray, V. *Biotechnol. Appl. Biochem.* **199**2, *15*, 303−310.
(24) (a) Katz, E.; Solov'ev, A. A. *J. Electroanal. Chem.* **1990**, *291*, 171−186. (b) Katz, E.; Schlereth, D. D.; Schmidt, H.-L. *J. Electroanal. Chem.* **1994**, *367*, 59−70. (c) Willner, I.; Riklin, A. *Anal. Chem.* **1994**, *66*, 1535−1539.

0.1 mM, in 0.1 M HEPES-buffer, pH 7.2, for 2 h, followed by rinsing with water. To produce the integrated COx/Cyt *c*-bioelectrocatalytic electrode for O_2 reduction,[25] the resulting Cyt *c*-modified electrode was interacted with cytochrome oxidase (COx), 0.5 mM, in TRIS-buffer, pH 8.0, for 2 h, washed briefly with water, and then treated with aqueous solution of glutaric dialdehyde, 10% v/v, for 30 min. The resulting modified electrode was washed with water.

Two types of electrochemical cells were constructed: one to perform cyclic voltammetry measurements and the second one to assemble biofuel cells. For the cyclic voltammetry measurements, the modified working electrodes (active area ca. 0.2 cm^2, roughness factor ca. 1.2) were introduced in an electrochemical cell that included a Pt-wire counter electrode and Ag-wire quasi-reference electrode. The quasi-reference electrode was calibrated[24b] according to the potential of dimethyl viologen, $E^\circ = -0.687$ V versus SCE, measured by cyclic voltammetry in a separate experiment, and the potentials are reported versus SCE. Biofuel cells were assembled from two modified electrodes (the reconstituted GOx/FAD-PQQ-electrode as an anode and the COx/Cyt *c*-electrode as a cathode or the integrated LDH/NAD^+-PQQ-electrode as an anode and the COx/Cyt *c*-electrode as a cathode; an active area of each electrode is ca. 0.2 cm^2, roughness factor ca. 1.2) that were sandwiched with a spacer providing a distance of 8 mm between the electrodes. Two plastic tubes (inlet and outlet) were added to the cell to convert the biofuel unit into a flow cell (flow rate 1 $mL \cdot min^{-1}$). A peristaltic pump was used to control the flow rate. Glucose or lactate solutions in 0.1 M TRIS-buffer, pH = 7.0, (in lactate, 10 mM $CaCl_2$ was added to the solution) saturated with air were applied to power the biofuel cells. The cell for cyclic voltammetry or the biofuel cell were inserted between the poles (diameter of 6 cm, separated by a distance of 1 cm) of an electromagnet (Model DPS-175, Scientific Equipment Roorkee, India) providing a constant magnetic field (±1% homogeneity) of variable strength that was measured with a Digital Gaussmeter (model DGM-102, manufactured by Sestechno, India). The cell (1-cm thick) was positioned between the centers of the poles. The images of the experimental setup and a diagram of the system are given as Supporting Information (S1). The modified biocatalytic electrodes were positioned parallel to the direction of the magnetic field. Electrochemical measurements were performed using an electrochemical analyzer (EG&G, VersaStat) linked to a computer (EG&G Software #270/250). Voltage and current produced by the biofuel cells were measured on a variable external resistance using an electrometer (Keithley 617). All the data were obtained at room temperature, ca. 24 ± 2 °C. Different magnetic fields applied on the electrochemical cell were generated by a sequential "ON" and "OFF" process.

A QCM analyzer (Fluke 164T multifunction counter, 1.3 GHz, TCXO) and quartz crystals (AT-cut, 9 MHz, Seiko) sandwiched between two Au electrodes (area 0.196 cm^2, roughness factor ca. 3.2) were employed for the microgravimetric analyses in air. The QCM crystals were calibrated by electropolymerization of aniline in 0.1 M H_2SO_4 and 0.5 M Na_2SO_4 electrolyte solution, followed by coulometric assay of the resulting polyaniline film and relating the crystal frequency changes to the electrochemically derived polymer mass.[26]

Theoretical Background

The mechanism of the magnetic field effect on mass-transport-limited electrochemical reactions will be discussed briefly. We limit our discussion considering only a constant homogeneous magnetic field applied parallel to the electrode surface plane. An electrochemical reaction occurring at the electrode surface yields a concentration gradient of the electroactive substrate along a diffusion layer of thickness, δ_D (Nernst approximation),[27] Scheme 1A. In the absence of magnetic field, the diffusion layer thickness is a function of the concentration, the diffusion coefficient of the substrate, and the electrode potential. Thus, at given values of these three parameters, we obtain a steady value of δ_D and a steady diffusion flux, $j = D(C^* - C_{el})/\delta_D$. As a result, the limiting current density generated in the system, $\boldsymbol{i}_L$, is governed by the δ_D value (assuming that the reactant concentration at the electrode surface $C_{el} = 0$), eq 1.[27]

Scheme 1. Schematic Illustration of the Mechanism for the Enhanced Mass Transport of Electroactive Species under an Applied Magnetic Field[a]

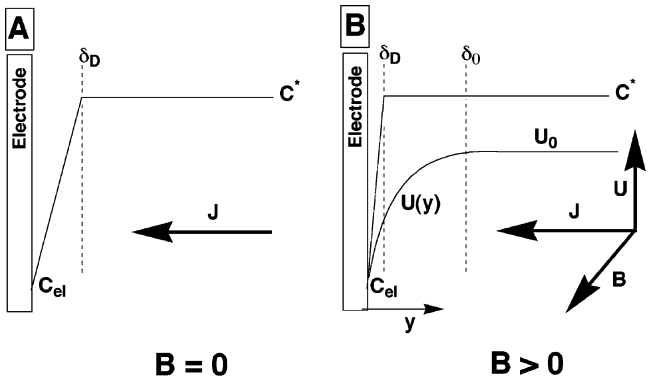

[a] J is the diffusional flux of the substrate, C_{el} is the substrate concentrations at the electrode surface, δ_D and δ_0 are the Nernst diffusion layer thickness and hydrodynamic boundary layer thickness, respectively, and U_0 is the fluid velocity on the outer edge of the hydrodynamic boundary layer.

$$\boldsymbol{i}_L = nFDC^*/\delta_D \quad (1)$$

where D is the diffusion coefficient, C^* corresponds to the concentration of the electroactive substrate in the bulk solution, n is the number of electrons per molecule involved in the redox process, and F is the Faraday constant**.**

Application of a magnetic field on a solution that includes moving ions (net current in our system) produces a magnetic body force, $\boldsymbol{F}_L$, acting on the system.[28] This force, $\boldsymbol{F}_L$, given by the Lorentz equation, eq 2, corresponds to the vector product of the net current density, $\boldsymbol{i}_L$, and the magnetic flux density, $\boldsymbol{B}$, that is exerted perpendicularly to these two vectors.[28]

$$\boldsymbol{F}_L = \boldsymbol{i}_L \times \boldsymbol{B} \quad (2)$$

The Lorentz force acts on the ions of the solution and results in a momentum transfer to the solvent. Under conditions where the flux of ions occurs orthogonal to the electrode surface and the applied magnetic field, $\boldsymbol{B}$, is directed parallel to the surface, the Lorentz force acts along the electrode surface. This leads to the formation of a solution flow, which is directed mainly tangential to the electrode surface and is present only under an applied magnetic field. This flow results in the formation of the hydrodynamic boundary layer of thickness δ_0 and a velocity gradient across this layer, Scheme 1B. The hydrodynamic flow results in the decrease of δ_D that leads to the accelerated mass transport of the electroactive species toward the electrode surface and to the enhanced electrochemistry. This leads to an increase in the current, I, through the bulk solution, resulting in the

(25) Pardo-Yissar, V.; Katz, E.; Willner, I.; Kotlyar, A. B.; Sanders, C.; Lill, H. *Faraday Discus.* **2000**, *116*, 119−134.
(26) Baba, A.; Tian, S.; Stefani, F.; Xia, C.; Wang, Z.; Advincula, R. C.; Johannsmann, D.; Knoll, W. *J. Electroanal. Chem.* **2004**, *562*, 95−103.
(27) Bockris, J. O'M.; Reddy, A. K. N.; Gamboa-Aldeco, M. *Modern Electrochemistry*; Plenum Press: New York, 1998.
(28) Kendall, P. C.; Plumpton, C. *Magnetohydrodynamics with Hydrodynamics*, Vol. 1; Pergamon Press: Oxford, 1964.

Scheme 2. Assembly of the Bioelectrocatalytic Electrodes[a]

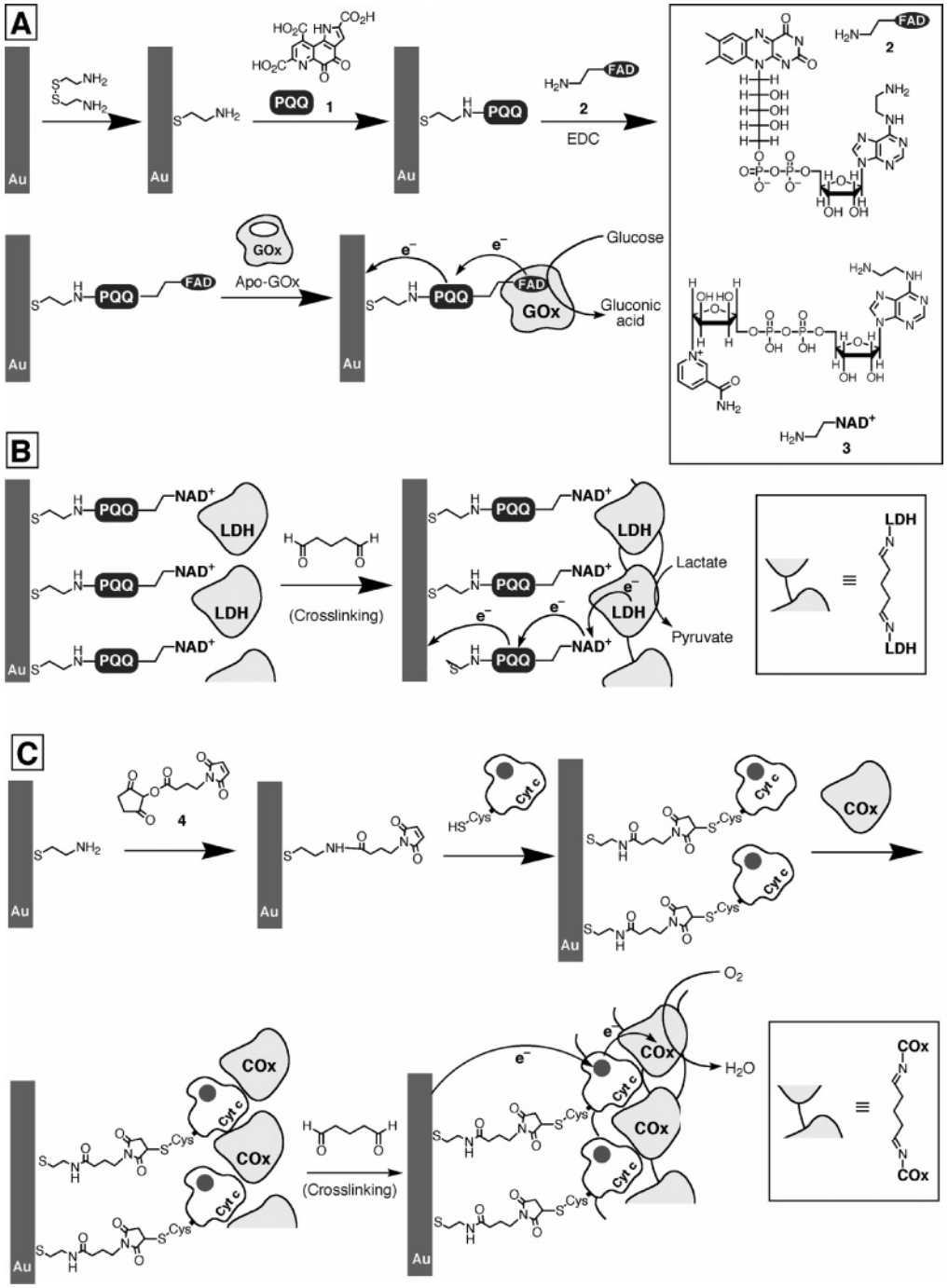

[a] (A) The glucose oxidase reconstitution on the FAD-PQQ self-assembled monolayer. (B) The lactic dehydrogenase association with the NAD^+-PQQ self-assembled monolayer followed by the enzyme cross-linking with glutaric dialdehyde. (C) The cytochrome oxidase association with the Cyt *c* self-assembled monolayer on the electrode followed by the enzyme cross-linking with glutaric dialdehyde.

increase in the flow velocity, and the further decrease of δ_D. This positive feedback mechanism is limited by dissipation in the boundary layer that results in the steady-state flow velocity and steady-state current. This phenomenon, known as the magnetohydrodynamic effect on electrochemical reactions, is experimentally documented in numerous studies.[17]

In a recent report, we formulated a theoretical model that accounts for the effects of a static homogeneous magnetic field, directed parallel to the planar semi-infinite electrode surface, on electrochemical reactions at interfaces.[18] In the development of the model, we used Levich relationship between the thickness of the Nernst diffusion layer, δ_D, and the thickness of the hydrodynamic boundary layer, δ_0.[29] For the flow moving over the plate, the thickness of the hydrodynamic boundary layer is inversely proportional to the square root of the flow velocity. The velocity of the arising flow depends on the applied magnetic flux density. As Levich[29] has shown that δ_D is proportional to δ_0, a decrease of the Nernst diffusion layer thickness is expected upon application of the magnetic field. Using the Navier−Stokes equation and the Nernst diffusion layer approximation,[27] we

(29) Levich, V. G. *Physicochemical Hydrodynamics*; Prentice Hall: Englewood Cliff, NJ, 1962.

formulated the relation between the limiting current of the redox-active substrate, the magnetic flux density, and the substrate concentration, as described in eq 3.[18]

$$\boldsymbol{i}_L = 0.63(\rho R)^{-1/3} D^{8/9} \nu^{-2/9} (nFC^*)^{4/3} B^{1/3} \qquad (3)$$

where n is the number of the electrons per molecule involved in the Faradaic process, F is the Faraday's number, R is an electrode characteristic size, ρ and ν are the fluid specific density and kinematic viscosity of the solution, respectively, D and C^* are the diffusion coefficient and the bulk concentration of the redox species, respectively, and B is the magnetic flux density (in Tesla). The expression (nFC^*) represents the value of the charge transferred across an electrode interface by a unit volume of the solution upon the electrochemical reaction. Hence, the body force acting on a unit volume of the solution and, accordingly, the resulting current, should be proportional to the n, F, and C^* in the same power, as was shown.

This theoretical model was successfully applied to analyze the magnetic field effects on simple electrochemical processes (e.g., the reduction of ferricyanide, the reduction of acetophenone, or the electrochemical deposition of Cu).[18,19(supporting information)] The limiting current, $\boldsymbol{i}_L$, of the electrochemical reaction at the interface is proportional to $B^{1/3}$ (for $C^* =$ constant). Furthermore, at a constant magnetic field, the limiting current relates to the concentration of the substrate according to the relation $\boldsymbol{i}_L \propto C^{*4/3}$.

An additional type of force acting on the electrolyte might arise from the magnetic field interactions with the ions in regions with a nonuniform concentration of ions. In the presence of a concentration gradient of ions, as a result of a redox reaction at an electrode, a force acting on paramagnetic or diamagnetic ions is generated.[30] This force has the same direction as the concentration gradient of the paramagnetic ions; orthogonal to the electrode surface, it linearly depends on the concentration gradient and does not depend on the direction of the magnetic field. As a result, an additional convective transport of all the components of the solution could be generated, resulting in further enhancement of the elecrochemical process.

Results and Discussions

Three bioelectrocatalytic systems were assembled on Au electrodes through multistep procedures outlined in Scheme 2. A gold electrode was initially modified with cystamine to yield an amino-group-functionalized surface, Scheme 2A. The resulting self-assembled monolayer provided an amine-functionalized interface for the covalent attachment of PQQ (**1**) that was then used for further covalent binding of N^6-(2-aminoethyl)-FAD cofactor (**2**), Scheme 2A, or N^6-(2-aminoethyl)-NAD^+ cofactor (**3**), Scheme 2B. Apo-glucose oxidase (apo-GOx) was reconstituted on the monolayer-immobilized FAD cofactor resulting in a biocatalytic interface for the oxidation of glucose, where the PQQ units served as mediators for the directional electron transfer from the FAD cofactor to the Au conductive support, Scheme 2A.[8a,b] Lactic dehydrogenase (LDH) was associated with the monolayer-immobilized NAD^+ cofactor by affinity cofactor−protein interactions, and the supramolecular structure was cross-linked with glutaric dialdehyde to yield the integrated biocatalytic matrix for the oxidation of lactate, Scheme 2B.[10a] The PQQ units in this structure serve as an electrocatalytic component for the oxidation of the biocatalytically generated NADH, thus providing a path for electron transfer from NADH to the conductive support and the regeneration of the NAD^+ cofactor for the continuous activation of the biocatalytic process. The third bioelectrocatalytic electrode was assembled by the covalent binding of the unique thiol group of iso-2-cytochrome *c* (Cyt *c*) to a maleimido monolayer-functionalized electrode surface, a process that led to the alignment of the redox protein, Scheme 2C.[25] The Cyt *c*-functionalized surface was reacted with the cytochrome oxidase (COx), resulting in the formation of the affinity complex between Cyt *c* and COx, which was further stabilized by cross-linking with glutaric dialdehyde to yield the integrated bioelectrocatalytic interface for the reduction of O_2 to H_2O. The Cyt *c* serves in this system as the specific electron-transfer mediator that stimulates vectorial electron transfer from the conductive support to COx.[25]

Table 1. Composition and Functional Properties of the Bioelectrocatalytic Electrodes

bioelectrocatalytic electrode	cofactor surface coverage[a] mole·cm^{-2}	enzyme surface coverage[a] mole·cm^{-2}	enzyme turnover[b] s^{-1}
GOx/FAD-PQQ	FAD 1.6×10^{-10}	GOx 2×10^{-12}	700
LDH/NAD^+-PQQ	NAD^+ 1.5×10^{-10}	LDH 7×10^{-12}	2.5
COx/Cyt *c*	Cyt *c* 8×10^{-12}	COx 2×10^{-12}	20

[a] The surface coverages of FAD and Cyt *c* were measured by cyclic voltammetry and QCM. The surface coverages of NAD^+, GOx, LDH, and COx were derived from QCM measurements. All surface coverages were calculated vs real electrode surface taking into account the electrode roughness factor (geometrical area ca. 0.2 cm^2, roughness factor ca. 1.2). The surface coverage of PQQ was 1.6×10^{-10} mole·cm^{-2}. [b] The GOx and LDH turnover numbers were derived from cyclic voltammetry measurements in the presence of the saturated substrate concentrations (glucose or lactate). The "turnover" number for COx was measured by cyclic voltammetry in the presence of O_2 concentration obtained in the equilibrium with air under normal pressure, and this number is below the enzyme saturation. The measurements were performed in the absence of magnetic field.

The bioelectrocatalytic electrodes, the reconstituted GOx/FAD-PQQ-electrode for the oxidation of glucose, the integrated LDH/NAD^+-PQQ-electrode for the oxidation of lactate, and the integrated COx/Cyt *c*-electrode for the reduction of oxygen, were characterized by cyclic voltammetry and quartz-crystal microbalance (QCM) measurements.[8a,b,10,15,25] The surface coverage values of the different biomolecules associated with the electrodes and the turnover numbers of the bioelectrocatalytic systems are summarized in Table 1. In the absence of magnetic field, the bioelectrocatalytic currents generated by the GOx/FAD-PQQ-electrode and by the LDH/NAD^+-PQQ-electrode reached the saturated levels at a glucose concentration of 80 mM and at a lactate concentration of 20 mM, respectively.

Cyclic voltammetry was used to follow and characterize the bioelectrocatalytic reactions stimulated by the enzyme-functionalized electrodes in the absence and in the presence of a constant magnetic field. Figure 1A, curve a, shows a background current of the reconstituted-GOx-electrode in the absence of glucose. The addition of glucose, 80 mM, results in the anodic bioelectrocatalytic current corresponding to the oxidation of glucose by the reconstituted-GOx system associated with the electrode surface, Figure 1A, curve b. Application of a constant magnetic field of $B = 0.92$ T (directed parallel to the electrode surface) results in an enhanced bioelectrocatalytic anodic current, Figure 1A, curve c. The cyclic voltammograms were recorded

(30) Hinds, G.; Coey, J. M. D.; Lyons, M. E. G. *Electrochem. Commun.* **2001**, *3*, 215−218.

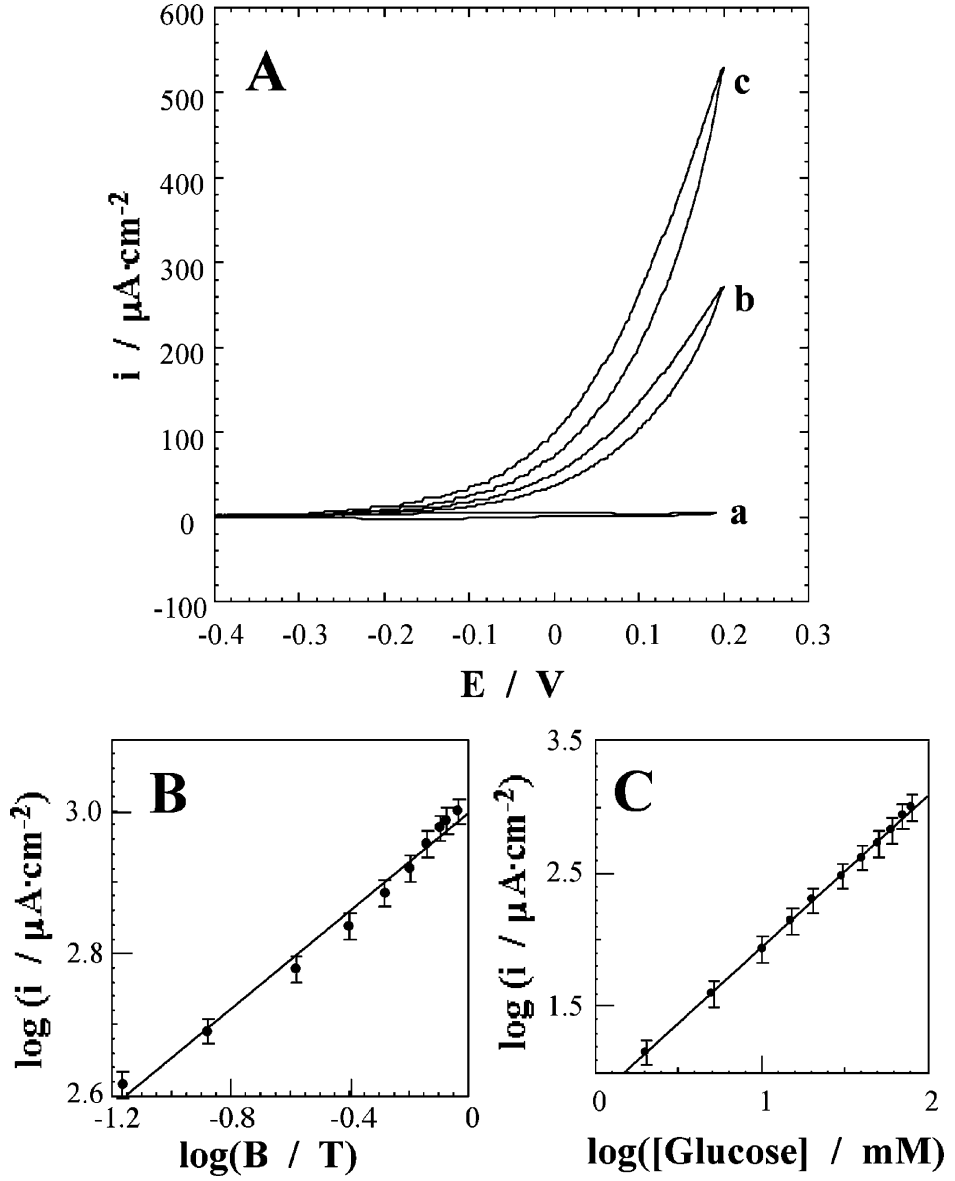

Figure 1. Effects of a constant magnetic field on the bioelectrocatalyzed oxidation of glucose by the GOx/FAD-PQQ-electrode. (A) Cyclic voltammograms measured on the electrode: (a) in the absence of glucose and in the absence of magnetic field; (b) in the presence of glucose, 80 mM, and in the absence of magnetic field; (c) in the presence of glucose, 80 mM, and in the presence of magnetic field, $B = 0.92$ T. (B) The dependence of the electrocatalytic current density on the magnetic flux density at glucose concentration of 80 mM. (C) The dependence of the electrocatalytic current density on the glucose concentration at an applied magnetic field corresponding to $B = 0.92$ T. The cyclic voltammograms were measured in 0.1 M TRIS-buffer, pH 7.0, potential scan rate 10 mV·s^{-1}. The electrocatalytic current densities are derived from the respective cyclic voltammograms at $E = 0.2$ V.

in the presence of variable concentrations of glucose, while applying a constant magnetic field corresponding to $B = 0.92$ T, and, similarly, the cyclic voltammograms were recorded upon applying different magnetic field intensities, while using a constant glucose concentration of 80 mM. These results were analyzed according to eq 3. The log $\boldsymbol{i}_L$ versus log B plot at a constant glucose concentration of 80 mM reveals a slope that corresponds to 0.343 ± 0.019 ($R^2 = 0.976$), as predicted by the model ($\boldsymbol{i}_L \propto B^{1/3}$), Figure 1B. The log $\boldsymbol{i}_L$ versus log C^* plot at a constant magnetic field of 0.92 T reveals a slope of 1.14 ± 0.01 ($R^2 = 0.999$), nearly as expected from the theoretical model ($\boldsymbol{i}_L \propto C^{*4/3}$), Figure 1C.

Figure 2A, curve a, shows a background cyclic voltammogram corresponding to the LDH/NAD$^+$-PQQ-integrated electrode in the absence of lactate. The addition of lactate, 20 mM, results in a bioelectrocatalytic anodic current corresponding to the oxidation of lactate by the LDH/NAD$^+$-PQQ-integrated system associated with the electrode, Figure 2A, curve b. Application of a constant magnetic field, $B = 0.92$ T results in the enhanced bioelectrocatalytic anodic current, Figure 2A, curve c. As before, the cyclic voltammograms were recorded in the presence of variable concentrations of lactate, while applying a constant magnetic field, $B = 0.92$ T, and upon the application of different magnetic field intensities, while using a constant lactate concentration of 20 mM. The results were analyzed according to eq 3. The log $\boldsymbol{i}_L$ versus log B plot at a constant lactate concentration of 20 mM reveals a slope that corresponds to 0.330 ± 0.043 ($R^2 = 0.959$), as predicted by the model ($\boldsymbol{i}_L \propto B^{1/3}$), Figure 2B. The log $\boldsymbol{i}_L$ versus log C^* plot at a constant magnetic field of 0.92 T reveals a slope of 1.04 ± 0.01 ($R^2 = 0.998$), which is smaller than the expected value from the theoretical model ($\boldsymbol{i}_L \propto C^{*4/3}$), Figure 2C. A possible reason

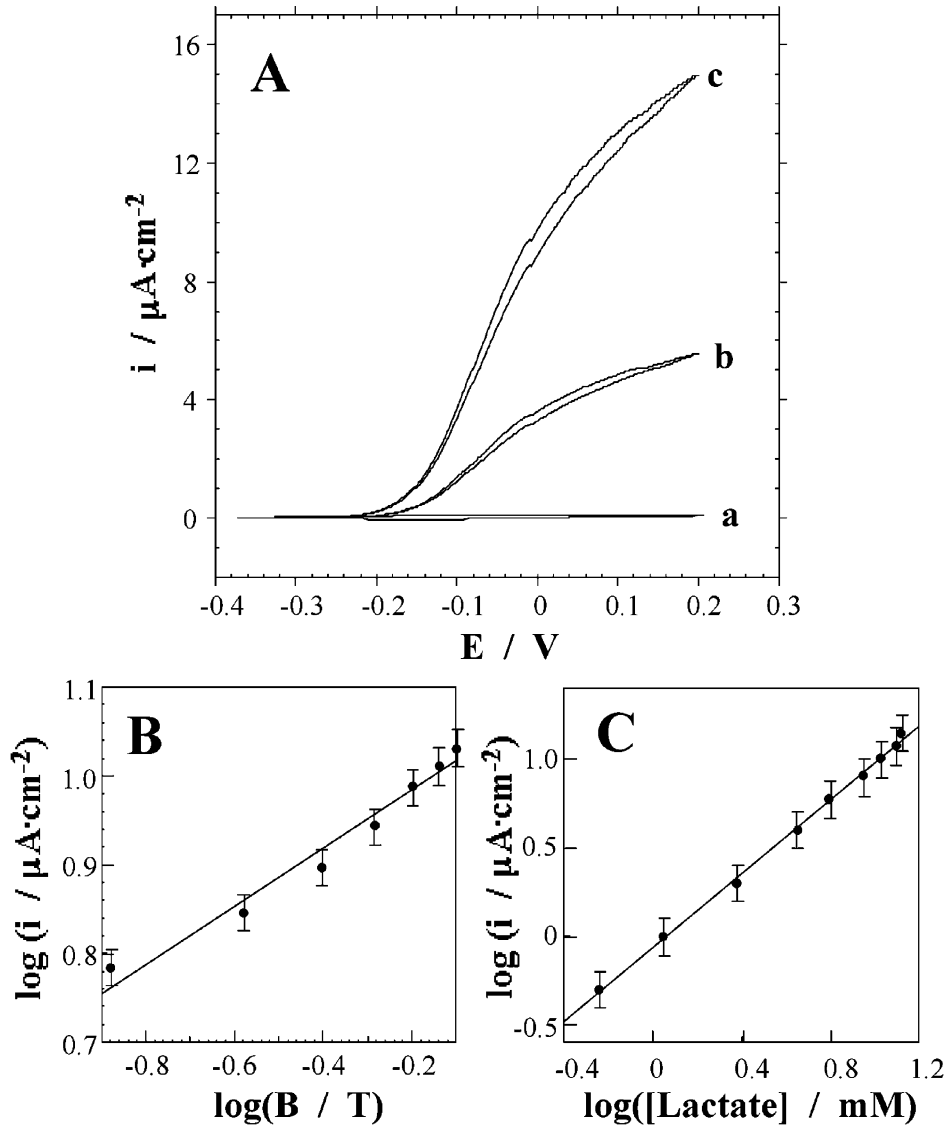

Figure 2. Effects of a constant magnetic field on the bioelectrocatalyzed oxidation of lactate by the LDH/NAD^+-PQQ-electrode. (A) Cyclic voltammograms measured at the electrode: (a) in the absence of lactate and in the absence of magnetic field; (b) in the presence of lactate, 20 mM, and in the absence of magnetic field; (c) in the presence of lactate, 20 mM, and in the presence of magnetic field, $B = 0.92$ T. (B) The dependence of the electrocatalytic current density on the magnetic flux density at lactate concentration of 20 mM. (C) The dependence of the electrocatalytic current density on the lactate concentration at an applied magnetic field of $B = 0.92$ T. The cyclic voltammograms were measured in 0.1 M TRIS-buffer, pH 7.0, containing $CaCl_2$, 10 mM, potential scan rate 10 $mV \cdot s^{-1}$. The electrocatalytic current densities are derived from the respective cyclic voltammograms at $E = 0.2$ V.

for this deviation from the theoretical model could be the fact that the LDH/NAD^+-PQQ-system is catalytically less effective than the reconstituted GOx system. Thus, the electrocatalytic oxidation of lactate may not be fully controlled by mass transport within the entire concentration region (the mass-transport limitation was the main assumption in the theoretical model).[18]

The application of a constant magnetic field in the direction perpendicular to the electrode surface showed only a minute effect on the bioelectrocatalytic anodic currents, probably because of an edge effect. These results imply that the enhanced bioelectrocatalytic anodic currents, indeed, originate from a Lorentz force exerted on the systems under the applied constant magnetic field parallel to the electrode surface.

The bioelectrocatalytic reduction of O_2 was studied by cyclic voltammetry using the COx/Cyt *c*-functionalized electrode. Figure 3, curve a, shows a background current on the COx/Cyt *c*-integrated electrode in the absence of O_2 (the air dissolved in the background electrolyte solution was removed by argon bubbling). The bioelectrocatalytic cathodic current corresponding to the reduction of O_2 by the COx/Cyt *c*-modified electrode is shown in Figure 3, curve b. Application of a constant magnetic field of $B = 0.92$ T (directed perpendicularly to the diffusion of O_2) results in the enhanced bioelectrocatalytic cathodic current, Figure 3, curve c. The observed increase in the bioelectrocatalytic current (ca. 30%) is smaller than that in the two bioelectrocatalytic oxidative systems (reconstituted GOx/FAD-PQQ-system and LDH/NAD^+-PQQ-integrated system). The magnetic effect on the electrochemical reduction of O_2 may originate from several possible mechanisms: The magnetohydrodynamic effect is possible assuming that the O_2 reduction on the electrode is at least partially limited by the mass-transport process.[31] An additional effect of magnetic field on the electrochemical reduction of O_2 was discussed in the literature,

(31) Kishioka, S.; Yamada, A.; Aogaki, R. *Elecroanalysis* **2001**, *13*, 1161−1164.

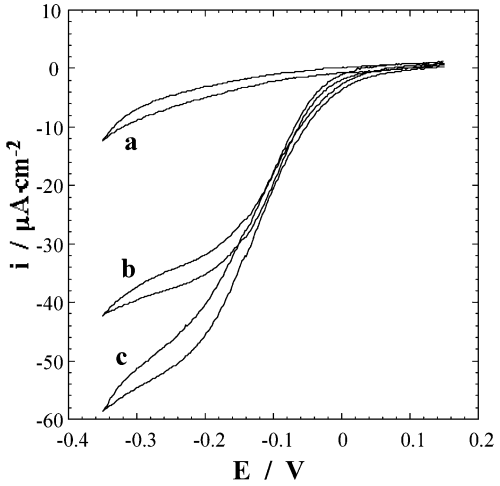

Figure 3. Cyclic voltammograms of the COx/Cyt *c*-electrode: (a) in the absence of oxygen (under Ar) and in the absence of a magnetic field; (b) in the presence of O_2 (under air) and in the absence of a magnetic field; (c) in the presence of O_2 (under air) and in the presence of a magnetic field, $B = 0.92$ T. The cyclic voltammograms were measured in 0.1 M TRIS-buffer, pH 7.0, potential scan rate 10 mV·s^{-1}.

and it originates from the paramagnetic properties of O_2 molecules.[30,32] Also, the O_2 solubility in water is increased in the presence of magnetic field, and this might further contribute to the enhancement of the bioelectrocatalytic process.[33] The complexity of the system does not allow us, however, to analyze quantitatively the magnetic field effect on the electrochemical process. One may conclude that all three bioelectrocatalytic processes that were examined in the presence of the modified electrodes are enhanced in the presence of the constant magnetic field, but the extent of the effect is dependent on the specific system.

The enhancement of the anodic and cathodic bioelectrocatalytic processes by the applied magnetic field brings us to the suggestion that the output of the biofuel cells consisting of bioelectrocatalytic electrodes may be improved under an applied magnetic field.[34] Two different configurations of the biofuel cells were constructed, and the magnetic field effects on them were studied. The first biofuel cell includes the biocatalytic anode based on the LDH/NAD^+-integrated electrode oxidizing lactate as a fuel and the bioelectrocatalytic cathode based on the COx/Cyt *c*-integrated electrode reducing O_2 as an electron acceptor, Scheme 3A. Figure 4A shows the voltage−current curves of the biofuel cell in the presence of 20 mM lactate solution saturated with air. The voltage−current curves were measured at variable loading resistances ($V_{cell} - i_{cell}$ loading function).[35] The loading functions of the biofuel cell measured in the absence and in the presence of the magnetic field, $B =$ 0.92 T, are shown in Figure 4A, curves a and b, respectively.

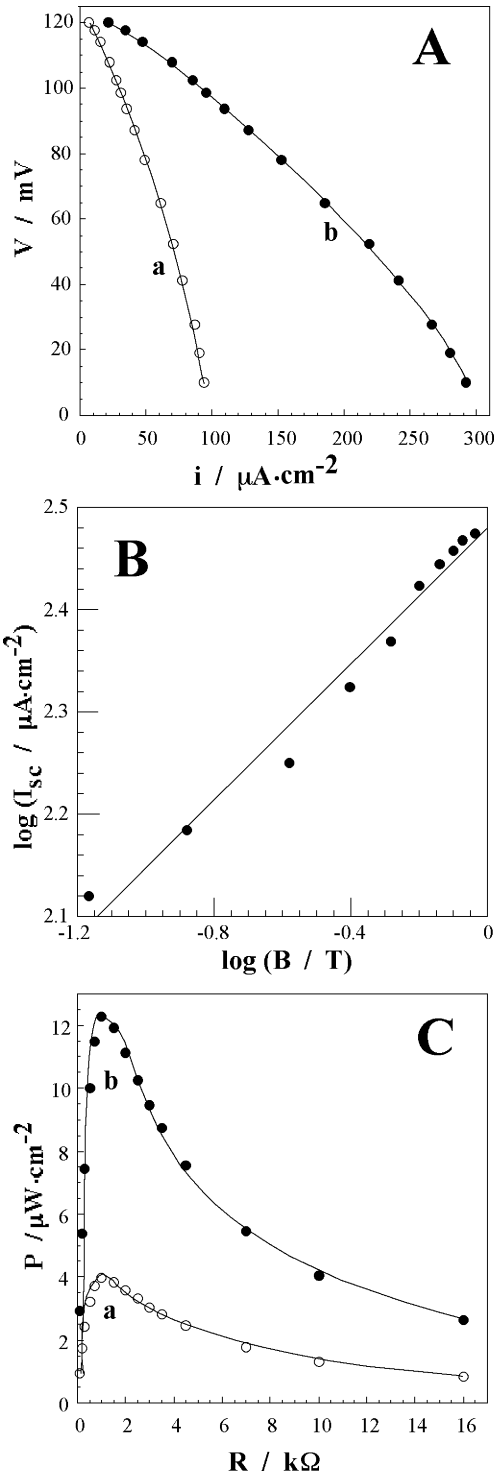

Figure 4. Enhancement of the performance of the biofuel cell composed of the LDH/NAD^+-PQQ-anode and COx/Cyt *c*-cathode: (A) The loading dependences measured at variable external resistances: (a) in the absence of magnetic field; (b) in the presence of magnetic field, $B = 0.92$ T. (B) The dependence of the short-circuit current density on the magnetic flux density. (C) The power density output generated by the biofuel cell: (a) in the absence of magnetic field; (b) in the presence of magnetic field, $B =$ 0.92 T. The biofuel cell operated upon pumping of the solution (flow rate 1 mL·min^{-1}) composed of 0.1 TRIS-buffer, pH 7.0, containing $CaCl_2$, 10 mM, lactate, 20 mM, and oxygen (the solution equilibrated with air).

The open-circuit voltage, V_{oc}, is ca. 120 mV and is independent of the applied magnetic field. This value corresponds to the maximum theoretical value[4d] determined by the difference of

(32) Rabah, K. L.; Chopart, J.-P.; Schloerb, H.; Saulnier, S.; Aaboubi, O.; Uhlemann, M.; Elmi, D.; Amblard, J. *J. Electroanal. Chem.* **2004**, *571*, 85−91.
(33) (a) Aogaki, R.; Kishioka, S. *Chem. Lett.* **1999**, 473−474. (b) Kishioka, S.; Yamada, A.; Aogaki, R.; Kiyoshi, T.; Goto, A.; Shimizu, T. *Chem. Lett.* **2000**, 656−657.
(34) Few reports have discussed the influence of a magnetic field on fuel cells performance (not biological). These reports do not deal, however, with the magnetohydrodynamic effect. Cf.: (a) Leddy, J.; Chung, H. In *39th Power Sources Proceedings*, **2000**, 144−147. (b) Okada, T.; Wakayama, N. I.; Wang, L. B.; Shingu, H.; Okano, J.; Ozawa, T. *Electrochim. Acta* **2003**, *48*, 531−539. (c) Leddy, J.; Zook, L. A.; Amarasinghe, S. U.S. Patent 6,-207,313,27 March 2001.
(35) Bockris, J. O'M.; Srinivasan, S. *Fuel Cells: Their Electrochemistry;* McGraw-Hill Book Company: New York, 1969.

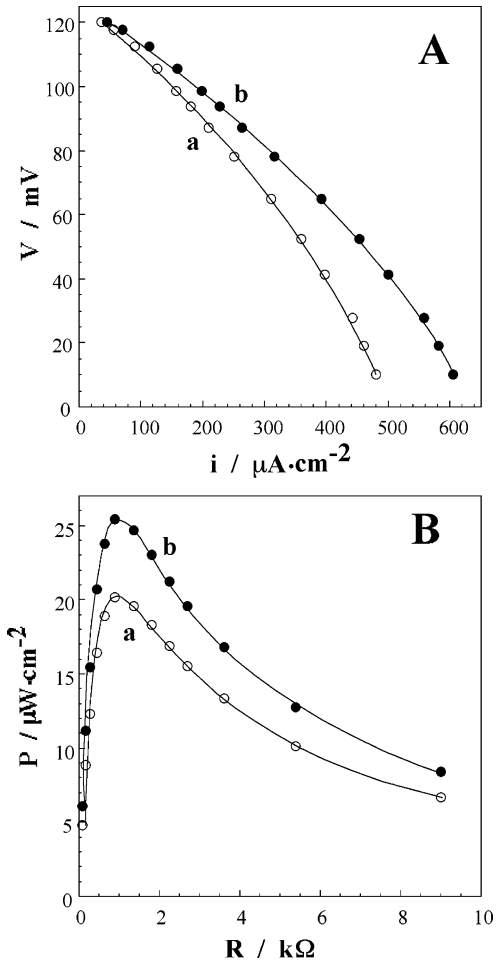

Figure 5. Enhancement of the performance of the biofuel cell composed of the GOx/FAD-PQQ-anode and COx/Cyt *c*-cathode: (A) The loading dependences measured at variable external resistances: (a) in the absence of magnetic field; (b) in the presence of magnetic field, $B = 0.92$ T. (B) The power density output generated by the biofuel cell: (a) in the absence of magnetic field; (b) in the presence of magnetic field, $B = 0.92$ T. The biofuel cell operated upon pumping of the solution (flow rate 1 mL·min^{-1}) composed of 0.1 TRIS-buffer, pH 7.0, containing glucose, 80 mM, and oxygen (the solution equilibrated with air).

the redox potentials of PQQ and Cyt *c* ($E_{PQQ}^{\circ} = -0.125$ V[24b] and $E_{Cyt}^{\circ} = 0.03$ V[25]), which mediate the electron-transfer processes between the biocatalyst units and the electrodes. It can be seen, however, that the applied constant magnetic field significantly affects the current density output of the biofuel cell. This is expected in view of the enhanced bioelectrocatalytic anodic current observed in the cyclic voltammetry experiment. The short-circuit current density, i_{sc}, increases from the value of ca. 100 μA·cm^{-2} in the absence of the magnetic field to the value of ca. 300 μA·cm^{-2} in the presence of the magnetic field, $B = 0.92$ T. The values of the short-circuit current density, i_{sc}, generated by the biofuel cell were measured at different magnetic fields, and the results were analyzed according to eq 3. The log i_{sc} versus log B plot at a constant lactate concentration of 20 mM and the saturated O_2 concentration reveals a slope that corresponds to 0.332 ± 0.041 ($R^2 = 0.988$), as predicted by the model ($i_L \propto B^{1/3}$), Figure 4B. The experimental value of the slope is though similar to the theoretically predicted value; even the system is composed of two bioelectrocatalytic electrodes and the O_2-reducing electrode could be affected by the magnetic field according to different possible mechanisms as discussed above. This originates from the fact that LDH/NAD$^+$-electrode exhibits a relatively low bioelectrocatalytic activity, and thus the lactate oxidation represents the limiting step in the overall process proceeding in the biofuel cell. The electrical power density output, $P = i \cdot V$, of the biofuel cell was plotted as a function of the external load resistance, R, Figure 4C. One can see that the power density output in the presence of the magnetic field, $B = 0.92$ T, Figure 4C, curve b, is substantially larger than that in the absence of the magnetic field, curve a. The maximum power output values in the absence and the presence of magnetic field, 4.1 μW·cm^{-2} and 12.4 μW·cm^{-2}, respectively, were observed at an external load resistance of $R = 1.2$ kΩ, indicating that the internal resistance of the biofuel cell is the same in the absence and upon application of the magnetic field. The ideal voltage−current relationship for an electrochemical generator is rectangular.[35,36] The experimental voltage−current density plots deviate from the rectangular shape, and the fill factor, $f = P_{max}/(i_{sc}V_{oc})^{-1}$, corresponds to ca. 0.34 in the absence as well as in the presence of the magnetic field. The small values of the fill factor and the voltage−current density dependence shape close to the linear function support the assumption that the electrochemical process in the biofuel cell is mass-transport limited, and thus the constant magnetic field leads to the enhanced power output as a result of the magnetohydrodynamic effect. The power output from the cell is, however, small and of limited practical utility. This low power output is due to several reasons that include a small potential difference between the mediator units associated with the anode and cathode, low turnover rates of the bioelectrocatalytic processes at the two electrodes, and the low current densities that originate from the monolayer configurations of the biocatalysts linked to the electrodes. Thus, the experiments and the results should be considered as a concept demonstrating the viability of an external magnetic field in enhancing biofuel cells performance. The same concept may be applied to other biofuel cells consisting of thin film-functionalized electrodes.[5f]

The second biofuel cell system that was studied included the GOx/FAD-PQQ-electrode as an anode for the oxidation of glucose and the COx/Cyt *c*-electrode as a cathode for the reduction of O_2, Scheme 3B. Figure 5A, curve a, shows the loading function, $V_{cell} - i_{cell}$, of the biofuel cell in the absence of magnetic field. Application of the magnetic field, $B = 0.92$ T, results in the enhancement of the current density output of the biofuel cell by ca. 30%, Figure 5A, curve b. The respective minor increase of the power density output in the presence of magnetic field is shown in Figure 5B, curves a and b, in the absence and the presence of magnetic field, $B = 0.92$ T, respectively. The smaller effect of the magnetic field on this biofuel cell originates from the fact that the oxygen-reducing COx/Cyt *c*-electrode exhibits lower biocatalytic activity as compared to the GOx/FAD-electrode. Thus, the O_2 reduction process that is the limiting step of the overall process controls the effect of the magnetic field on the power output of the biofuel cell. Since the O_2 bioelectrocatalytic cathodic reaction is only slightly affected by the magnetic field, the total effect of magnetic field on the biofuel cell process is determined by the small enhancement of the cathodic process.

(36) Erdey-Gruz, T. *Kinetics of Electrode Processes*; Adam Hilger: London, 1972; pp 133−141.

Scheme 3. Configurations of the Biofuel Cells on the Basis of (A) Lactate-Oxidizing LDH/NAD^+-PQQ-Electrode as an Anode and O_2-Reducing COx/Cyt *c*-Electrode as a Cathode. (B) Glucose-Oxidizing GOx/FAD-PQQ-Electrode as an Anode and O_2-Reducing COx/Cyt *c*-Electrode as a Cathode

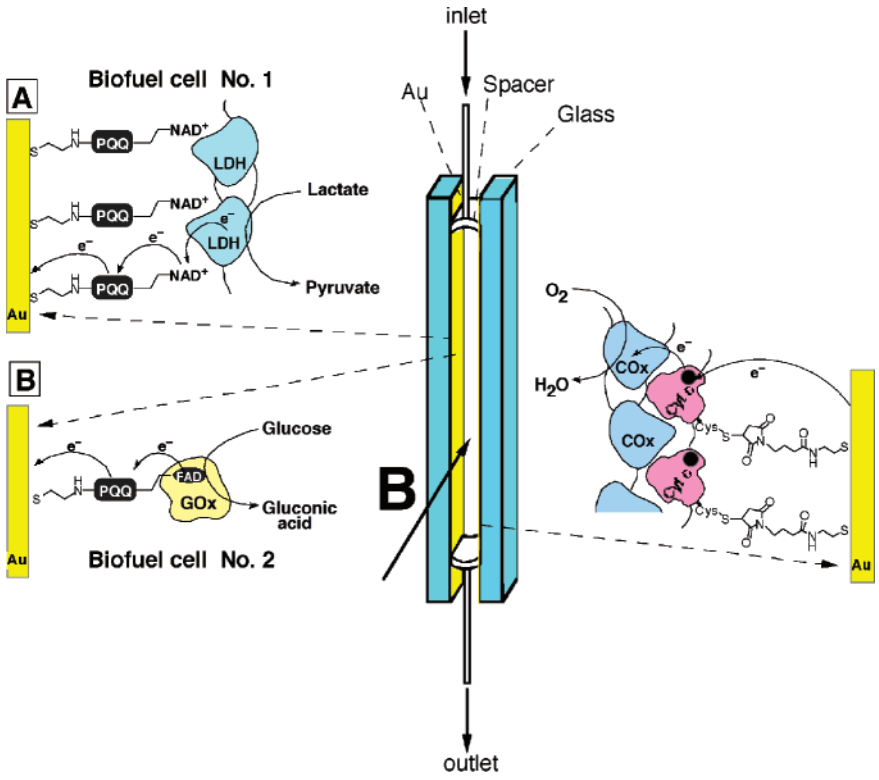

Conclusions

The study has described the effects of a constant magnetic field (applied parallel to the electrode surface) on surface-confined bioelectrocatalytic systems associated with electrodes. Specifically, we found pronounced magnetic field effects on the bioelectrocatalytic oxidation of glucose and the bioelectrocatalytic oxidation of lactate by the reconstituted GOx electrode and a structurally organized LDH/NAD^+-PQQ electrode, respectively. The results were nicely correlated with a magnetohydrodynamic model that was formulated by us. A small magnetic field effect was demonstrated for the bioelectrocatalytic reduction of O_2 by an integrated COx/Cyt *c*-electrode. The magnetic field effect on this system is, at present, mechanistically unclear. Besides the general biochemical implications of the results that might shed light on the magnetic field effects on biocatalytic electron-transfer reactions occurring at membrane interfaces, we demonstrated the utility of the magnetohydrodynamic effect for enhancing the power output of biofuel cells. A 3-fold increase in the power output of the LDH/NAD^+-PQQ||COx/Cyt *c* cell was observed at a magnetic field of 0.92 T and an external load of 1.2 kΩ. Our results indicate that one has to search for the magnetic field effects on the electrode that controls the power output of the biofuel cells to improve the biofuel cell performance. Other biofuel cell configurations, such as the use of a laccase cathode, are being examined. However, the magnetic field effect on the biofuel cell performance should be observed for mass-transport-limited systems. For biofuel cells that do not meet this condition, the magnetic field effect should be negligible.

Acknowledgment. This research is supported by the Israel Science Foundation.

Supporting Information Available: The images of the experimental setup and a diagram of the system are given as Supporting Information (S1). This material is available free of charge via the Internet at http://pubs.acs.org.

JA044157T